Parallel Implementation of the Discrete Green's Function Formulation of the FDTD Method on a Multicore Central Processing Unit

Tomasz STEFAŃSKI[1], *Sławomir ORŁOWSKI*[1], *Bartosz REICHEL*[2]

[1]Faculty of Electronics, Telecommunications and Informatics, Gdansk University of Technology, Narutowicza 11/12, 80-233 Gdansk, Poland
[2]Faculty of Applied Physics and Mathematics, Gdansk University of Technology, Narutowicza 11/12, 80-233 Gdansk, Poland

tomasz.stefanski@pg.gda.pl, orlowski.slawomir@gmail.com, reichel@mif.pg.gda.pl

Abstract. *Parallel implementation of the discrete Green's function formulation of the finite-difference time-domain (DGF-FDTD) method was developed on a multicore central processing unit. DGF-FDTD avoids computations of the electromagnetic field in free-space cells and does not require domain termination by absorbing boundary conditions. Computed DGF-FDTD solutions are compatible with the FDTD grid enabling the perfect hybridization of FDTD with the use of time-domain integral equation methods. The developed implementation can be applied to simulations of antenna characteristics. For the sake of example, arrays of Yagi-Uda antennas were simulated with the use of parallel DGF-FDTD. The efficiency of parallel computations was investigated as a function of the number of current elements in the FDTD grid. Although the developed method does not apply the fast Fourier transform for convolution computations, advantages stemming from the application of DGF-FDTD instead of FDTD can be demonstrated for one-dimensional wire antennas when simulation results are post-processed by the near-to-far-field transformation.*

Keywords

Computational electromagnetics, discrete Green's function (DGF), finite-difference time-domain (FDTD) method, parallel processing.

1. Introduction

Recently, several computational techniques facilitating the finite-difference time-domain (FDTD) method [1] were developed based on the discrete Green's function (DGF) [2], [3], [4], [5]. DGF is the impulse response of a system of finite-difference equations defined on a discrete domain. The convolution of DGF with current sources exciting that domain allows to obtain the FDTD solution without execution of the standard FDTD update procedure throughout the entire domain. Moreover, DGF-based computations do not need absorbing boundary conditions (ABCs) for simulations of the radiation and scattering problems in the FDTD grid. Therefore, DGF has been applied to FDTD simulations of antennas with savings in runtime and memory usage [6], [7], [8], [9].

In [6], the DGF-based scattering formulation of the FDTD method (DGF-FDTD) was developed for antenna simulations. It computes currents at conducting surfaces with the use of the march-on-in-time scheme (i.e., the evolution of antenna currents is computed one time step at a time based on currents computed for previous time steps). Similarly to the FDTD method, DGF-FDTD allows to obtain wideband frequency characteristics of an antenna in a single simulation run. Although DGF-FDTD solves the time-domain electric field integral equation, it is inherently discrete and the whole formulation is much more straightforward in comparison to other methods based on time-domain integral equations [9].

Recently, DGF-FDTD has been coupled with the FDTD method [10], [11], hence consistent with the discrete theory of electromagnetism hybridization of FDTD was developed. Because FDTD solutions have their own dispersion, anisotropy, and stability properties, the coupling of FDTD and integral-equation methods requires discrete equivalents to the integral operator and the Green's function (i.e., DGF) [4]. Using FDTD method hybridized with DGF, simulation scenarios involving interacting transmitters and scatterers can be tackled without computations of the field in free-space cells between these objects. Moreover, the transmitters and scatterers can be simulated separately and a system response can be obtained in terms of the diakoptics approach (i.e., as a response of interacting multi-port subsystems) [12]. Currently, commercial FDTD solvers allow running two-stage simulations with the source of radiation simulated at the first stage and multiple simulations of the irradiation at the second stage [13]. Hence, many different

objects weakly coupled with the source of radiation can be simulated with savings in runtime. Such FDTD simulations, as well as other applications of the diakoptics in the FDTD method, can take advantage of DGF-FDTD.

In spite of the mentioned above advantages of the DGF-FDTD method, its parallel implementations on modern computing architectures, such as multicore central processing units (CPUs) and graphics processing units (GPUs), have attracted little attention so far. Therefore, the parallel implementation of the DGF-FDTD method on CPU was developed. It has recently been reported that the application of the fast Fourier transform (FFT) for spatial convolution computations leads to favorable throughput of DGF-FDTD compared to the standard FDTD method [8]. The presented here parallel DGF-FDTD implementation does not employ FFT for acceleration of the convolution computations. In spite of that, advantages due to the application of DGF-FDTD instead of FDTD can be demonstrated for one-dimensional wire antennas (especially when simulation results are post-processed by the near-to-far-field (NTFF) transformation).

2. DGF-FDTD Method

The DGF-FDTD method represents FDTD update equations by means of the convolution of the current sources ($\mathbf{J}$, $\mathbf{M}$) and dyadic DGF ($\mathbf{G_{ee}}$, $\mathbf{G_{eh}}$, $\mathbf{G_{he}}$, $\mathbf{G_{hh}}$) [6]:

$$\begin{bmatrix} \mathbf{E}\,|^{n}_{ijk} \\ \eta\mathbf{H}\,|^{n}_{ijk} \end{bmatrix} = \sum_{n'i'j'k'} \begin{bmatrix} \mathbf{G_{ee}}\,|^{n-n'}_{i-i'j-j'k-k'} & \mathbf{G_{eh}}\,|^{n-n'}_{i-i'j-j'k-k'} \\ \mathbf{G_{he}}\,|^{n-n'}_{i-i'j-j'k-k'} & \mathbf{G_{hh}}\,|^{n-n'}_{i-i'j-j'k-k'} \end{bmatrix} \begin{bmatrix} \eta\mathbf{J_{eq}}\,|^{n'}_{i'j'k'} \\ \mathbf{M_{eq}}\,|^{n'}_{i'j'k'} \end{bmatrix} \tag{1}$$

where:

$$\mathbf{J_{eq}}\,|^{n}_{ijk} = (s_x s_y s_z)^{-1} c\Delta t \mathbf{J}\,|^{n}_{ijk}, \tag{2}$$

$$\mathbf{M_{eq}}\,|^{n}_{ijk} = (s_x s_y s_z)^{-1} c\Delta t \mathbf{M}\,|^{n}_{ijk}\,. \tag{3}$$

In (1)–(3), $s_p = c\Delta t/\Delta p$ denotes the Courant number, c is the speed of light, Δt is the time-step size, Δp is the discretization-step size along the p-direction ($p = x, y, z$), η is the intrinsic impedance of free space, n is the time index, and i, j, k are the spatial indices in the grid. Equation (1) is referred to as the convolution formulation of the FDTD method [6]. If the length of DGF waveforms is equal to the number of time steps in the FDTD simulation, this formulation returns the same results as the direct FDTD method (assuming infinite numerical precision of computations).

Only the $\mathbf{G_{ee}}$ component of DGF is presented here for the sake of brevity. Its analytic closed-form expression in infinite free space takes the following form for the (i, j, k) cell [5]:

$$G_{ee,xz}\,|^{n}_{ijk} = \sum_{m=\alpha_x+\beta_x+\gamma_x}^{n-2} \binom{n+m}{2m+2} g_{xz}\,|^{m}_{ijk}, \tag{4}$$

$$G_{ee,yz}\,|^{n}_{ijk} = \sum_{m=\alpha_y+\beta_y+\gamma_y}^{n-2} \binom{n+m}{2m+2} g_{yz}\,|^{m}_{ijk}, \tag{5}$$

$$\begin{aligned} G_{ee,zz}\,|^{n}_{ijk} = {} & -s_x s_y s_z U\,|^{n-1}\,\delta\,|_{ijk} + \\ & \sum_{m=max(\alpha_{f,z}+\beta_{f,z}+\gamma_{f,z}-1,0)}^{n-2} \binom{n+m}{2m+2} f_{zz}\,|^{m+1}_{ijk} + \\ & \sum_{m=\alpha_{h,z}+\beta_{h,z}+\gamma_{h,z}}^{n-2} \binom{n+m}{2m+2} h_{zz}\,|^{m}_{ijk} \end{aligned} \tag{6}$$

where:

$$\begin{aligned} g_{xz}\,|^{m}_{ijk} = {} & -(-1)^{m+i+j+k} \sum_{\substack{\alpha+\beta+\gamma=m \\ \alpha\geqslant\alpha_x,\beta\geqslant\beta_x,\gamma\geqslant\gamma_x}} \binom{m}{\alpha,\beta,\gamma} \times \\ & \binom{2\alpha+1}{\alpha+i+1} \binom{2\beta}{\beta+j} \binom{2\gamma+1}{\gamma+k} s_x^{2\alpha+2} s_y^{2\beta+1} s_z^{2\gamma+2}, \end{aligned} \tag{7}$$

$$\begin{aligned} g_{yz}\,|^{m}_{ijk} = {} & -(-1)^{m+i+j+k} \sum_{\substack{\alpha+\beta+\gamma=m \\ \alpha\geqslant\alpha_y,\beta\geqslant\beta_y,\gamma\geqslant\gamma_y}} \binom{m}{\alpha,\beta,\gamma} \times \\ & \binom{2\alpha}{\alpha+i} \binom{2\beta+1}{\beta+j+1} \binom{2\gamma+1}{\gamma+k} s_x^{2\alpha+1} s_y^{2\beta+2} s_z^{2\gamma+2}, \end{aligned} \tag{8}$$

$$\begin{aligned} f_{zz}\,|^{m}_{ijk} = {} & -(-1)^{m+i+j+k} \sum_{\substack{\alpha+\beta+\gamma=m \\ \alpha\geqslant\alpha_{f,z},\beta\geqslant\beta_{f,z},\gamma\geqslant\gamma_{f,z}}} \binom{m}{\alpha,\beta,\gamma} \times \\ & \binom{2\alpha}{\alpha+i} \binom{2\beta}{\beta+j} \binom{2\gamma}{\gamma+k} s_x^{2\alpha+1} s_y^{2\beta+1} s_z^{2\gamma+1}, \end{aligned} \tag{9}$$

$$\begin{aligned} h_{zz}\,|^{m}_{ijk} = {} & -(-1)^{m+i+j+k} \sum_{\substack{\alpha+\beta+\gamma=m \\ \alpha\geqslant\alpha_{h,z},\beta\geqslant\beta_{h,z},\gamma\geqslant\gamma_{h,z}}} \binom{m}{\alpha,\beta,\gamma} \times \\ & \binom{2\alpha}{\alpha+i} \binom{2\beta}{\beta+j} \binom{2\gamma+2}{\gamma+k+1} s_x^{2\alpha+1} s_y^{2\beta+1} s_z^{2\gamma+3}. \end{aligned} \tag{10}$$

Other terms denote: $\alpha_x = \max(-i-1, i)$, $\beta_x = |j|$, $\gamma_x = \max(-k, k-1)$, $\alpha_y = |i|$, $\beta_y = \max(j, -j-1)$, $\gamma_y = \max(-k, k-1)$, $\alpha_{f,z} = \alpha_{h,z} = |i|$, $\beta_{f,z} = \beta_{h,z} = |j|$, $\gamma_{f,z} = |k|$, $\gamma_{h,z} = \max(|k|-1, 0)$. $U\,|^{n}$ and $\delta\,|_{ijk}$ respectively denote the unit step and Kronecker delta functions. Expressions for other $\mathbf{G_{ee}}$ components can be obtained rotating the subscripts x, y, z and the corresponding summation indices.

Let us consider an antenna made of a perfect electric conductor (PEC) simulated inside the FDTD grid. For nodes in the grid belonging to PEC, the total electric field is equal to zero:

$$E_p^{total}\,|^{n}_{ijk} = E_p^{inc}\,|^{n}_{ijk} + E_p^{scat}\,|^{n}_{ijk} = 0 \quad (i, j, k, p) \in PEC \tag{11}$$

where E^{total}, E^{inc} and E^{scat} denote respectively total, incident and scattered electric field. (i, j, k, p) denotes the p-component of the field belonging to the (i, j, k) cell in the

grid. With the use of (1), the scattered electric field can be obtained from currents induced on the antenna due to the incidence of the electric field:

$$E_p^{scat}\,|_{ijk}^{n} = \sum_{(i',j',k',p')\in PEC} \sum_{n'=0}^{n-1} G_{ee,pp'}\,|_{i-i'j-j'k-k'}^{n-n'}\,\eta(J_{eq})_{p'}\,|_{i'j'k'}^{n'}\,. \tag{12}$$

Then, the equation relating the incident electric field and currents induced on the antenna can be obtained using (11)–(12):

$$E_p^{inc}\,|_{ijk}^{n} = -\frac{\Delta t}{\varepsilon_0} \sum_{(i',j',k',p')\in PEC} \sum_{n'=0}^{n-1} G_{ee,pp'}\,|_{i-i'j-j'k-k'}^{n-n'}\,(s_x s_y s_z)^{-1} J_{p'}\,|_{i'j'k'}^{n'} \tag{13}$$

where $(i,j,k,p) \in PEC$. For $n = 1$, the $\mathbf{G_{ee}}$ component of DGF (4)–(6) reduces to:

$$\mathbf{G_{ee}}\,|_{ijk} = -(s_x s_y s_z)\delta\,|_{ijk}\,\mathbf{I} \tag{14}$$

where $\mathbf{I} = \mathrm{diag}(1,1,1)$ denotes the unit dyad. Hence, one obtains from (13) the time-marching procedure for computations of the time evolution of the antenna currents based on the incident electric field:

$$J_p\,|_{ijk}^{n-1} = \frac{\varepsilon_0}{\Delta t} E_p^{inc}\,|_{ijk}^{n} + \sum_{(i',j',k',p')\in PEC} \sum_{n'=0}^{n-2} G_{ee,pp'}\,|_{i-i'j-j'k-k'}^{n-n'}\,(s_x s_y s_z)^{-1} J_{p'}\,|_{i'j'k'}^{n'}\,. \tag{15}$$

These antenna currents can be employed for computations of radiation characteristics. In the developed code, the NTFF transformation is implemented based on formulation [1]. However, the far-field pattern is computed directly from the antenna currents. Therefore, for the NTFF computations, savings in runtime and memory usage are obtained in comparison to FDTD because the DGF-FDTD method does not need to employ the equivalence principle at a closed surface enclosing the antenna. Moreover, the computed antenna currents can be employed for excitation of the total-field scattered-field interface in FDTD simulations [11].

3. Parallel DGF-FDTD Solver

The method was implemented in double precision using the C programming language. A single iteration of the time-marching procedure of the developed parallel DGF-FDTD solver is implemented as presented in Fig. 1. In the parallel DGF-FDTD implementation, all tasks are executed by a set of parallel CPU threads. The OpenMP parallel programming standard was employed for implementation of the algorithm in software.

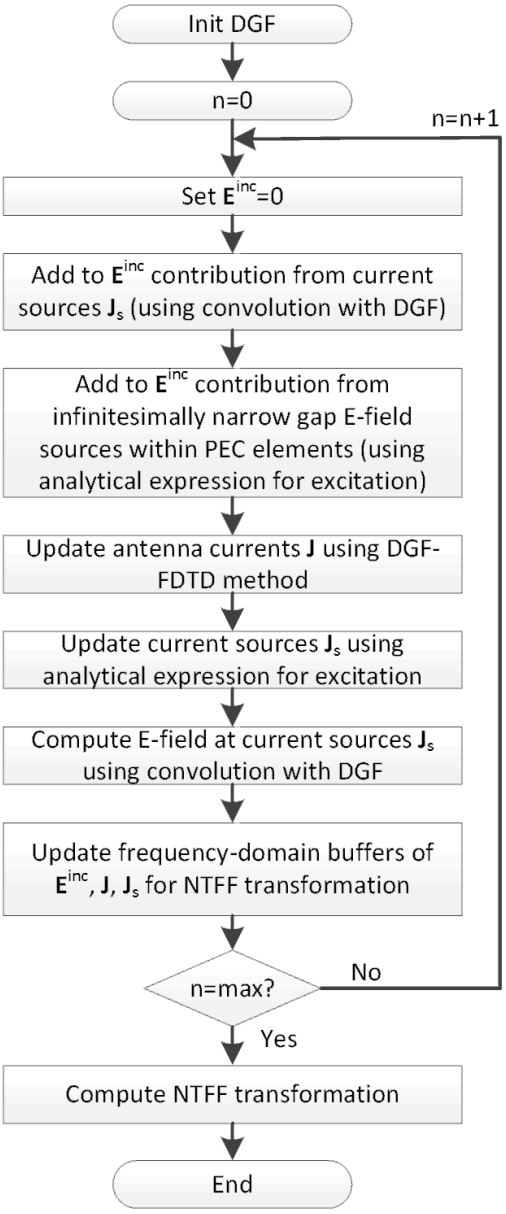

Fig. 1. Flowchart of the developed algorithm.

A single iteration of the time-marching procedure of the parallel DGF-FDTD method is implemented as follows (refer to Fig. 1):

- Buffer of the electric field incident at PEC elements ($\mathbf{E}^{inc}$) is set to zero with the use of parallel threads.
- Contributions to $\mathbf{E}^{inc}$ from current sources feeding the antenna are computed in parallel for each PEC element.
- Contributions to $\mathbf{E}^{inc}$ from infinitesimally narrow gap sources within PEC elements are computed in parallel for each PEC element.
- The DGF-FDTD update procedure (15) is executed in parallel for each PEC element.
- The current sources feeding the antenna are updated in parallel for each source.

- The electric field measured at the current sources feeding the antenna is computed in parallel for each source.
- The frequency-domain buffers for the NTFF transformation are updated in parallel for each PEC element and current source.

The method requires the generation of DGF waveforms (the init DGF step) corresponding to the currents at the antenna. The DGF generation is a part of the pre-processing stage or, alternatively, the DGF waveforms can be read from a file on a hard drive. Unfortunately, the DGF generation currently requires significant processor time. In the developed parallel DGF-FDTD solver, the hardware accelerated methods of the DGF generation [14], [15], [16] are available for antenna simulations. Although the DGF generation is an active topic of research in computational electromagnetics, these computations still remain a bottleneck for applications of the DGF-FDTD method. Therefore, DGF waveforms are truncated to speed up computations, and the windowing technique [17] is applicable for increasing the accuracy of results. However, such an approximation of DGF deteriorates the compatibility of DGF-FDTD with the direct FDTD method. Alternatively, the approximation of dyadic DGF can be obtained from scalar DGF by the truncation of scalar DGF when this function approaches zero (i.e., the steady state). This idea was already employed in the DGF-FDTD simulations [9] with the use of the DGF formulation derived based on scalar DGF [6]. In the developed solver, dyadic DGF is generated from (4)–(10) without intermediate computations of scalar DGF. Therefore, the latter approach to the DGF generation [9] cannot currently be applied in our DGF-FDTD solver. If the accuracy or stability of the DGF-FDTD computations is not satisfactory, then increasing the DGF window length is a solution to these problems. Finally, taking DGF waveforms whose length is equal to the number of time steps in a simulation always assures the same results as returned by the direct FDTD method.

The runtime scaling of the DGF-FDTD convolution computations executed over M PEC elements is of order $(M^2 n_s)$, where n_s denotes the DGF length (computational cost of the DGF generation is excluded from consideration). On the other hand, the direct FDTD computations require to update all cells in the three-dimensional domain containing the antenna. The runtime scaling of these computations is of order (N^3), where N^3 denotes the number of cells in a cubic domain. Therefore, the efficiency of the DGF-FDTD method is higher than the direct FDTD method if a small number of sparsely distributed PEC elements is simulated within a large domain.

For the sake of comparison, simulated antennas can be fed from electric current sources. The developed DGF-FDTD method can employ the one-cell gap model of source, similarly to the direct FDTD method, instead of the infinitesimally narrow gap model [18]. For this purpose, the computations of the incident electric field in the DGF-FDTD method [6] were modified to include contributions from such current sources. As a result of simulation, the developed solver returns FDTD-compatible waveforms of the incident electric field and the antenna currents as well as far-field radiation patterns.

A graphical user interface (GUI) was developed for the DGF-FDTD solver, refer to Fig. 2, and integrated with the in-house written FDTD simulation tool [19]. It facilitates the edition of simulation parameters, drawing PEC elements, running simulations, and the presentation of results. The developed GUI also provides other functionalities that help in preparing and running DGF-FDTD simulations. In the developed GUI code, the OpenGL library was employed for visualization of computational domain and simulation results. It allows to place PEC elements into the domain, as well as rotate, shift and scale visualized objects. The architecture of the developed software package simplifies the development of its new features by using well defined design patterns along with own engine for data management [19].

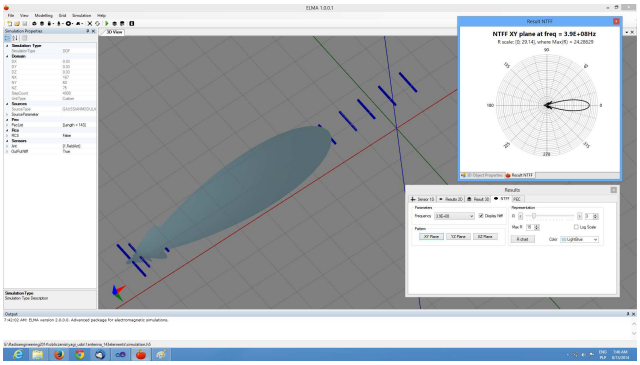

Fig. 2. GUI of the developed simulation tool.

4. Numerical Results

The method was tested on a machine with Intel i7-3770 3.4 GHz processor. The Courant numbers were taken as $s_x = s_y = s_z = 0.99/\sqrt{3}$ for the results presented here. In the presented investigations, the DGF waveforms were read from a file on a hard drive.

Fig. 3(a) presents comparison between waveforms computed with the use of DGF-FDTD and FDTD for a square loop antenna. It consists of 44 current elements (43 PEC elements and a current source at the feeding point). The spatial discretization in this simulation was taken as $\Delta x = \Delta y = \Delta z = 1$ mm. The number of time steps in the simulation was set to 600, which was equal to the DGF length. It allows to verify the correctness of the DGF-FDTD implementation for the DGF waveforms which are not distorted by the windowing. In this test, the size of FDTD domain in the reference simulation was sufficient to avoid reflections from imperfect ABC. The harmonic current source excited the antenna with the frequency set to 6.81 GHz. Fig. 3(b) presents the error between both methods. The correctness of the DGF-FDTD computations is validated by the error varying in the range -300 to -260 dB.

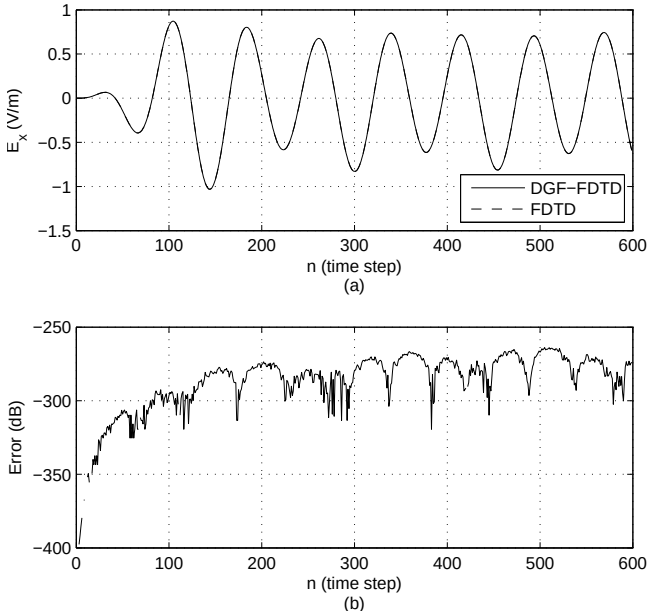

Fig. 3. (a) Electric field waveforms computed at the feeding point of the loop antenna simulated with the use of DGF-FDTD and FDTD. (b) Relative error between both methods. Discontinuity of the line means that both methods computed exactly the same result in double precision.

Arrays of Yagi-Uda antennas were considered for the sake of benchmarking of the parallel code. The spatial discretization in these simulations was taken as $\Delta x = \Delta y = \Delta z =$ 3 cm. A single array element consisting of 143 current elements is presented in Fig. 4. The following configurations of antennas in the two-dimensional arrays were considered: 1×2, 1×3, 1×4, 2×3, 2×4. The distances between antennas in arrays were uniformly set to 24 cells. The modulated harmonic current source excited each antenna in arrays with the frequency band set to 350–450 MHz. The uniform amplitude and equal phase distributions were considered in the simulation scenario. The NTFF transformation was computed with the step size set to 1° for discrete polar and azimuthal angles. The number of time steps in simulations was set to 4000, whereas the DGF waveforms were truncated using the Hann's window with the length set to $n_s = 400$ samples. Such simulation parameters allowed to obtain stable and satisfactorily accurate results. However, parameters of the DGF truncation cannot be fixed and always depend on the simulated problem. Since the DGF waveforms were read from a file on a hard drive, the presented computing runtimes are independent of the methods of the DGF generation and truncation.

The correctness of the antenna-array simulations was verified by a comparison to the results of direct FDTD computations. For this purpose, characteristics of a single array element were computed. In Fig. 5, the comparison between electric field waveforms computed at the feeding point of a single Yagi-Uda antenna, simulated using DGF-FDTD and FDTD, is presented. As seen, waveforms simulated using the DGF-FDTD and FDTD methods overlap as long as the time step is less than n_s. It shows that the DGF length equal to the number of time steps in a simulation allows to obtain results overlapping with results of the direct FDTD method. In Fig. 6, the comparison between far-field patterns computed using DGF-FDTD and FDTD is presented for a single Yagi-Uda antenna. As seen, the far-field patterns computed using the DGF-FDTD and FDTD methods overlap for simulation parameters taken as described above. The differences between DGF-FDTD and FDTD are insignificant, although FDTD employs the NTFF transformation implemented with the use of a single Huygens surface [1], [20]. The obtained results validate the correctness of the parallel implementation of DGF-FDTD in software.

In Fig. 7, execution runtimes are presented as a function of the number of current elements in the simulated antenna arrays. Runtimes were measured for the DGF-FDTD update loop, the NTFF transformation that is outside of the DGF-FDTD update loop, as well as the total execution runtimes of the code were measured. For the sake of comparison, results measured for the serial DGF-FDTD code are also presented. The developed parallel DGF-FDTD implementation is maximally 4.3 times faster than its serial implementation (2×4 array, 1144 current elements) when the total execution runtimes are compared. It is a satisfactory result for the code executed on CPU with 4 cores and 8 threads (hyper threading).

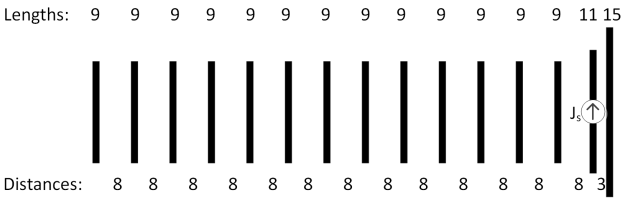

Fig. 4. Geometry of the Yagi-Uda antenna being an element of the considered antenna arrays (distances and lengths measured in grid cells).

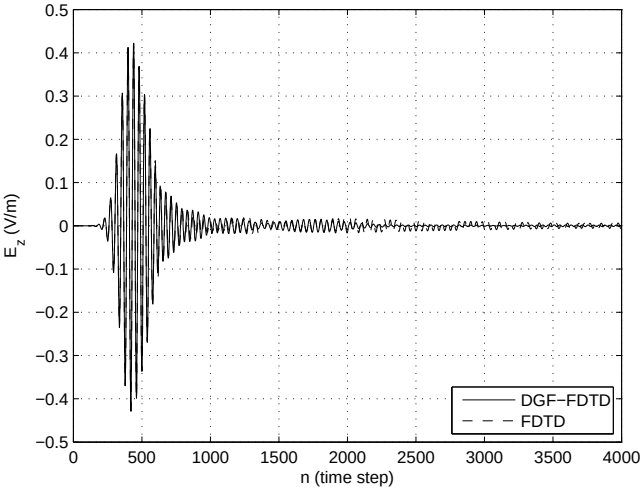

Fig. 5. Electric field waveforms computed at the feeding point of a single Yagi-Uda antenna.

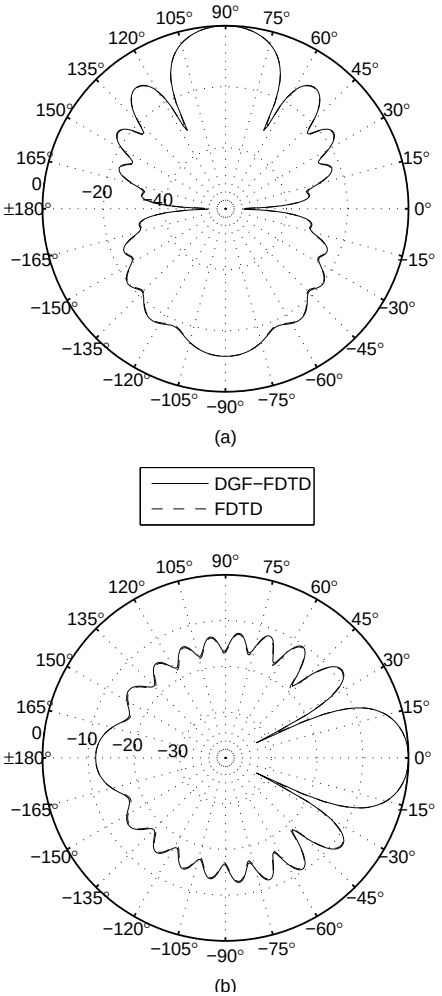

Fig. 6. Exemplary far-field patterns computed for a single Yagi-Uda antenna (values in dB, frequency of NTFF transformation was set to 390 MHz). (a) E-plane. (b) H-plane.

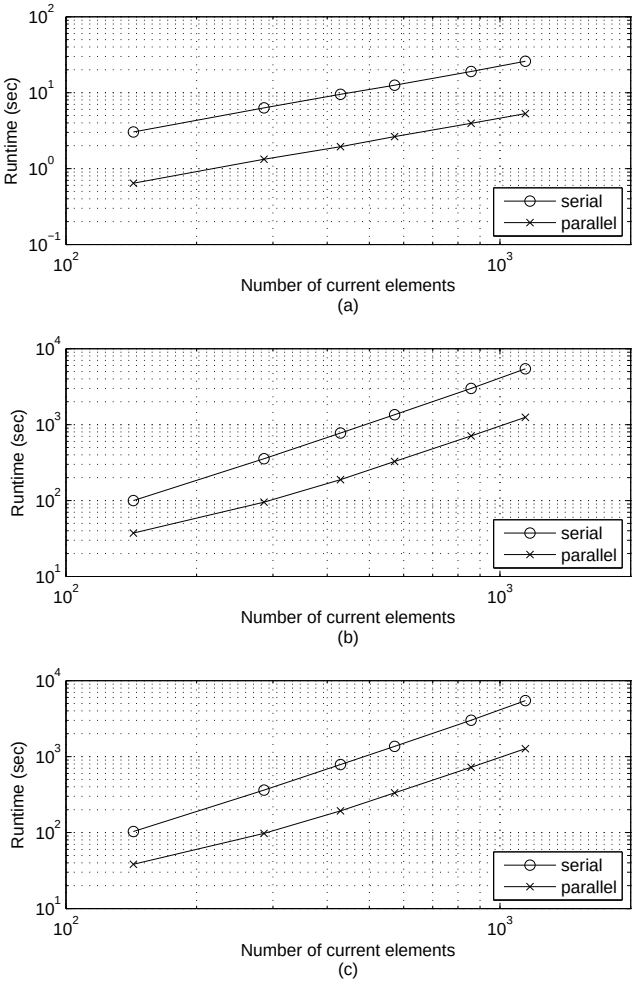

Fig. 7. Execution runtimes for serial and parallel implementations of the DGF-FDTD method. (a) Runtime of NTFF transformation. (b) Runtime of update loop. (c) Total execution runtime.

Execution runtimes were compared between DGF-FDTD and FDTD. Although the developed method does not apply FFT for convolution computations [8], advantages due to the application of DGF-FDTD instead of FDTD can be demonstrated for the considered one-dimensional wire antennas when simulation results are post-processed by the NTFF transformation. In the FDTD method, the standard NTFF transformation employs the Huygens surface whose area depends on the volume of the computational domain. On the other hand, DGF-FDTD computes the NTFF transformation from current sources feeding the antenna and currents induced on antenna wires. For a large number of observation points in the far-field zone, the NTFF computations may take significant processor time in FDTD. Therefore, DGF-FDTD was faster than FDTD in the presented tests for small antenna arrays. For instance, DGF-FDTD was maximally 5.9 times faster than FDTD for a single Yagi-Uda antenna (143 current elements). However, FDTD was faster than DGF-FDTD for 2×3 and 2×4 arrays (858 and 1144 current elements, respectively). Fortunately, the convolution computations can be accelerated using FFT, hence additional speedup of the DGF-FDTD method can still be obtained.

5. Conclusions

The parallel DGF-FDTD method was implemented on multicore CPU. The method is applicable to simulations of wire antennas made of PEC. Computed DGF-FDTD solutions are compatible with the FDTD grid enabling the perfect hybridization of FDTD with the use of time-domain integral equation methods. The computational efficiency of the developed parallel DGF-FDTD solver was investigated in antenna simulations. Although the developed method does not apply FFT for convolution computations, advantages due to the application of DGF-FDTD instead of FDTD can be demonstrated for one-dimensional antennas when simulation results are post-processed by the NTFF transformation. The presented implementation represents the intermediate step in the process of development of the accelerated DGF-FDTD solver executable on heterogeneous parallel processing systems. This topic is planned to be reported in the future.

Acknowledgments

This work was supported by the Polish National Science Center under Agreement DEC-2012/05/D/ST7/00141.

References

[1] TAFLOVE, A., HAGNESS, S. C. *Computational Electrodynamics: The Finite-Difference Time-Domain Method*, 3rd ed. Boston (USA): Artech House, 2005.

[2] VAZQUEZ, J., PARINI, C. G. Discrete Green's function formulation of FDTD method for electromagnetic modelling. *Electronics Letters*, 1999, vol. 35, no. 7, p. 554 - 555.

[3] HOLTZMAN, R., KASTNER, R. The time-domain discrete Green's function method (GFM) characterizing the FDTD grid boundary. *IEEE Transactions on Antennas and Propagation*, 2001, vol. 49, no. 7, p. 1079 - 1093.

[4] KASTNER, R. A multidimensional z-transform evaluation of the discrete finite difference time domain Green's function. *IEEE Transactions on Antennas and Propagation*, 2006, vol. 54, no. 4, p. 1215 - 1222.

[5] JENG, S.-K. An analytical expression for 3-D dyadic FDTD-compatible Green's function in infinite free space via z-transform and partial difference operators. *IEEE Transactions on Antennas and Propagation*, 2011, vol. 59, no. 4, p. 1347 - 1355.

[6] MA, W., RAYNER, M. R., PARINI, C. G. Discrete Green's function formulation of the FDTD method and its application in antenna modeling. *IEEE Transactions on Antennas and Propagation*, 2005, vol. 53, no. 1, p. 339 - 346.

[7] HOLTZMAN, R., KASTNER, R., HEYMAN, E., ZIOLKOWSKI, R. W. Ultra-wideband cylindrical antenna design using the Green's function method (GFM) as an absorbing boundary condition (ABC) and the radiated field propagator in a genetic optimization. *Microwave and Optical Technology Letters*, 2006, vol. 48, no. 2, p. 348 - 354.

[8] MIRHADI, S., SOLEIMANI, M., ABDOLALI, A. An FFT-based approach in acceleration of discrete Green's function method for antenna analysis. *Progress In Electromagnetics Research M*, 2013, vol. 29, p. 17 - 28.

[9] MIRHADI, S., SOLEIMANI, M., ABDOLALI, A. UWB antennas analysis using FDTD-based discrete Green's function approach. *IEEE Antennas and Wireless Propagation Letters*, 2013, vol. 12, p. 1089 - 1093.

[10] STEFAŃSKI, T. P. Hybrid technique combining the FDTD method and its convolution formulation based on the discrete Green's function. *IEEE Antennas and Wireless Propagation Letters*, 2013, vol. 12, p. 1448 - 1451.

[11] STEFAŃSKI, T. P. Application of the discrete Green's function-based antenna simulations for excitation of the total-field/scattered-field interface in the FDTD method. *Microwave and Optical Technology Letters*, 2014, vol. 56, no. 8, p. 1949 - 1953.

[12] DE HON, B. P., ARNOLD, J. M. Stable FDTD on disjoint domains - a discrete Green's function diakoptics approach. *Proceedings of the Second European Conference on Antennas and Propagation.* Edinburgh (UK), 2007, p. 1 - 6.

[13] BENKLER, S., CHAVANNES, N., KUSTER, N. Novel FDTD Huygens source enables highly complex simulation scenarios on ordinary PCs. *Proceedings of the IEEE Antennas and Propagation Society International Symposium.* Charleston (SC, USA), 2009, p. 1 - 4.

[14] STEFAŃSKI, T. P. Fast implementation of FDTD-compatible Green's function on multicore processor. *IEEE Antennas and Wireless Propagation Letters*, 2012, vol. 11, p. 81 - 84.

[15] STEFAŃSKI, T. P., KRZYŻANOWSKA, K. Implementation of FDTD-compatible Green's function on graphics processing unit. *IEEE Antennas and Wireless Propagation Letters*, 2012, vol. 11, p. 1422 - 1425.

[16] STEFAŃSKI, T. P. Implementation of FDTD-compatible Green's function on heterogeneous CPU-GPU parallel processing system. *Progress In Electromagnetics Research*, 2013, vol. 135, p. 297 - 316.

[17] STEFAŃSKI, T. P. Accuracy of the discrete Green's function formulation of the FDTD method. *IEEE Transactions on Antennas and Propagation*, 2013, vol. 61, no. 2, p. 829 - 835.

[18] WATANABE, S., TAKI, M. An improved FDTD model for the feeding gap of a thin-wire antenna. *IEEE Microwave and Guided Wave Letters*, 1998, vol. 8, no. 4, p. 152 - 154.

[19] ORŁOWSKI, S., STEFAŃSKI, T. P. Development of graphical user interface for modern FDTD simulation tool. In *Proceedings of the Progress in Electromagnetics Research Symposium.* Stockholm (Sweden), 2013, p. 1210 - 1214.

[20] MARTIN, T. An improved near- to far-zone transformation for the finite-difference time-domain method. *IEEE Transactions on Antennas and Propagation*, 1998, vol. 46, no. 9, p. 1263 - 1271.

About Authors...

Tomasz STEFAŃSKI received the M.Sc. degree in telecommunications and the Ph.D. degree in electronics engineering, from Gdansk University of Technology (GUT), Gdansk, Poland, in 2002 and 2007, respectively. He is currently leading projects founded by the Foundation for Polish Science and the National Science Center at the Faculty of Electronics, Telecommunications and Informatics at GUT. Before joining GUT in 2011, he was with the Swiss Federal Institute of Technology (ETH Zurich) conducting research on parallelization of electromagnetic solvers on modern computing architectures using OpenCL programming language. Between 2006 and 2009 he worked at the University of Glasgow developing parallel alternating direction implicit finite-difference time-domain (ADI-FDTD) full-wave solvers for general purpose high-performance computers and graphics processing units. His current research interests include computational electromagnetics, parallel processing and microwave engineering.

Sławomir ORŁOWSKI received the M.Sc. degree and the Ph.D. degree in physics from Nicolaus Copernicus University (NCU), Torun, Poland, in 2004 and 2009, respectively. He is currently working in research projects at the Faculty of Electronics, Telecommunications and Informatics at Gdansk University of Technology, Gdansk, Poland. Between 2008 and 2010 he worked at NCU developing software tools for optical coherence tomography. His current research interests include computational electromagnetics, software design, computer graphics, image and signal processing.

Bartosz REICHEL received the M.Sc degree in applied physics and the Ph.D. degree in theoretical physics from

Gdansk University of Technology (GUT), Gdansk, Poland, in 2004 and 2008, respectively. He is currently an Assistant Professor at the Faculty of Applied Physics and Mathematics at GUT. Since 2013, he is involved in research projects at the Faculty of Electronics, Telecommunications and Informatics at GUT focusing on computational electromagnetics and optimization of algorithms on graphics processing units. Between 2004 and 2008 he worked toward the Ph.D. degree investigating the propagation of short light pulses in waveguides. His current research interests include computational electromagnetics, parallel processing and electromagnetic scattering.